TJ

Institut de Physique Nucléaire de Lyon

Université Claude Bernard

IN2P3 - CNRS

LYCEN 2000/32
March 2000

Compton scattering off polarized electrons with a high finesse Fabry-Pérot cavity at JLab

N. Falletto, et Al.
J-M. Mackowski, L. Pinard

Submitted to NIM B

43, Boulevard du 11 Novembre 1918 - 69622 VILLEURBANNE Cedex - France

Compton Scattering off polarized electrons with a High Finesse Fabry-Pérot Cavity at JLab

N. Falletto, M. Authier, G. Bardin, M. Baylac, M. Boyer, F. Bugeon, E. Burtin, C. Cavata, N. Colombel, G. Congretel, R. Coquillard, G. Coulloux, B. Couzy, P. Deck, A. Delbart [1], D. Desforges, A. Donati, B. Duboué, S. Escoffier, F. Farci, B. Frois, P. Girardot, J. Guillotau, C. Henriot, J. Jardillier, C. Jeanney, M. Julliard, J-P. Jorda, P. Legou, D. Lhuillier, Y. Lussignol, Ph. Mangeot, X. Martin, F. Marie, J. Martino, F. Maurier, B. Mazeau, J.F. Millot, F. Molinié, J-P. Mols, J-P. Mouly, M. Mur, D. Neyret, T. Pédrol, S. Platchkov, G. Pontet, T. Pussieux, Y. Queinec , Ph. Rebourgeard, J. C. Sellier, G. Tarte, C. Veyssière, A. Zakarian,

DAPNIA CEA Saclay, 91191 Gif/Yvette Cedex, France.

P. Bertin,

LPC/IN2P3, Clermont Ferrand, France.

J. Mitchell,

Thomas Jefferson National Accelerator Facility, Newport News, VA 23606, USA.

J-M. Mackowski and L. Pinard,

IPNL/IN2P3, Université Claude Bernard Lyon I, 69622 Villeurbanne cedex, France.

Abstract

We built and operated a new kind of Compton polarimeter to measure the electron beam polarization of the Thomas Jefferson National Accelerator Facility (Virginia, USA). The heart of this polarimeter is a High Finesse monolithic Fabry-Pérot cavity. Its purpose is to amplify a primary 300 mW laser beam to improve the signal to noise ratio of the polarimeter. It is the first time that a High Finesse Fabry-Pérot cavity

Preprint submitted to Elsevier Preprint *25 February 2000*

is enclosed in the vacuum of a particle accelerator to monitor the beam polarization by Compton polarimetry. The measured Finesse and amplification gain of the cavity are $F = 26000$ and $G = 7300$. The electron beam crosses this high power photon source with an angle of 23 mrad at the middle of cavity where the photon beam power density is estimated to be 0.85 MW/cm^2. We have used this facility during the HAPPEX experiment (April-July 1999) and we give a preliminary measurement of the Compton scattering experimental asymmetry.

1 Introduction

A large fraction of the physics program at Jefferson Lab [1] uses polarized electrons of energy between 1 and 8 GeV and for beam current up to 100 μA. These experiments require a measurement of the electron beam polarization with an accuracy better than 3% and with a monitoring of its time dependant variations. This can be achieved by using Compton scattering polarimetry which is used elsewhere either at a higher current [2] or at a higher energy [3],[4]. For the experimental conditions of Jlab, we built and operated a Compton polarimeter which uses a high Finesse Fabry-Pérot cavity as a high power photon source [5,6]. This is the first Fabry-Pérot cavity coupled to the beam pipe of an electron accelerator to measure and monitor the polarization of an electron beam used for nuclear physics experiments.

This polarimeter is described on figure 1. The electron beam is deflected in a 4-dipole magnetic chicane. Polarized electrons of the accelerator beam scatter off circularly polarized photons stored in the cavity which is located between the second and third dipoles. The Fabry-Perot cavity amplifies a 300mW Continuous Wave (CW) Nd:Yag laser beam (λ=1064 nm). It is enclosed in the electron beam pipe of the chicane. The energy of backscattered photons is measured in a $PbWO_4$ calorimeter and a silicon microstrip detector is currently commissioned to measure the momentum of scattered electrons. The photon polarization is measured at the exit of the optical cavity.

In this paper, we report on the installation and the commissionning of this Compton polarimeter. We describe the experimental set-up with a focus on the optical cavity. We then give the measured performances of the photon source and we show the evidences of the Compton scattering signal. Finally, we give a preliminary analysis of data taken during the HAPPEX experiment at a beam energy of E=3.355 GeV and a beam current of $I_e = 40\mu$ A.

[1] Corresponding author. Tel.: +33 1 69083454; e-mail: adelbart@cea.fr

2 The TJNAF Hall A Compton Polarimeter

The aim of this section is to describe the main components of the Compton polarimeter (see figure 1). The photon beam and its injection in the Fabry-Pérot cavity is the purpose of the next section.

2.1 The magnetic chicane and the associated vacuum system

For a photon energy of $k = 1.165$ eV, the scattered photons of energy k greater than 40 MeV are emitted in a 350 μrad cone around the electron beam. The magnetic chicane (figure 2) deflects the electron beam in the lower pipe to cross the photon beam and allows the scattered photons to be detected. The 4 dipoles of the chicane are identical and are associated in series to return the electron beam to the hall A experiment without altering its direction, energy and polarization.

The vertical displacement of the beam in the central lower beam line is necessary to get the crossing of the electron and photon beams. This is achieved by slightly adjusting the field of the dipoles. The position of the beam is controlled with downstream and upstream Beam Position Monitors (BPM) and the background level is monitored with 4 Beam Diagnostics, each made of 4 scintillators read by PMTs.

Every part of the polarimeter beam line was optimized to ensure a low pressure and clean vacuum at the CIP and thus reduce as much as possible the Bremsstrahlung radiation seen by the photon detector. The cleanliness is required to keep the cavity mirrors out of any pollution which would lower the cavity build-up gain. Because of the higher pressure in the beam pipe downstream of the polarimeter ($\approx 10^{-7}$ Torr), we use seven ionic pumps for an overall pumping power of 480 l/s. The mechanical spacer of the cavity was also designed to optimize the pumping. Although the stainless steel components in contact with the vacuum were baked at 1000 °C during several hours, the desorbtion of the other materials within the lower beam line can explain the 10^{-8} Torr vacuum observed with the electron beam going through.

With a proper tuning of the electron beam, we were able to lower the overall background counting rate below $0.6kHz/\mu$A for the nominal electron beam of HAPPEX (see section 4).

The scattered photons are detected and their energy is measured in a photon calorimeter made of 5x5 $PbWO_4$ scintillators. Each crystal is 20x20x230 mm^3 and is read at one side by a Philips XP1911 photomultiplier tube. The crystals are enclosed in a 16 ^oC thermostated box because of the light yield sensitivity to temperature ($2\%/^oC$).

Lead tungstate crystal was chosen for its high density (8.28 g/cm^3), small Molière radius (2.19 cm), fast response (62% of the charge in 100 ns) and good radiation hardness. The calorimeter is thus compact and its dead time minimized. An energy resolution of $\frac{\sigma(E)}{E} = 1.76\% \oplus \frac{2.75\%}{\sqrt{E}} \oplus \frac{0.41\%}{E}$ was measured on Mainz tagged photon beam line [9].

The data acquisition system of the Compton polarimeter was designed to collect the photon calorimeter signals at the 100kHz Compton counting rate and to monitor the beams' parameters at a frequency up to 600 Hz.

After amplification, the photomultipliers signals are used to generate a trigger for the photon acquisition system, and these signals are integrated and measured by 10 fast ADC cards. To reach the requested counting rate, these ADCs are bufferized and read by blocks (10MB/s maximum data flux on VME bus). Then these values are attributed to each electron beam polarization pulse (30 Hz rate), and some calculations (photon energy histogrammation) are processed by two different PowerPC CPUs.

In parallel, the electron and photon beam parameters are monitored at 600 Hz rate and attributed to each polarization pulse. These data are then stored in the same file on a Sun workstation.

3 The photon beam and its amplification by the High Finesse Fabry-Pérot cavity

The laser and all the optical components are aligned on three different breadboards for ease of maintenance procedures. These breadboards are mounted on a vibration-isolated honeycomb table (see figure 3) which also supports the lower central beam pipe containing the optical cavity and the vacuum pumps and gauges. The overall opto-electronic system is controlled and commanded from the hall A counting room via the EPICS control system [10](figure 4). The optical setup is described on figure 6.

The following conditions are required to get the Fabry-Pérot power build-up :

- the stability parameter must first verify $-1 \leq g = 1 - \frac{L}{R} \leq 1$ where L is the cavity length and R is the radius of curvature of the mirrors,
- the two mirrors must be accurately aligned and oriented one with respect to the other to avoid diffraction losses,
- the frequency of the input laser has to be locked on a resonant frequency of the cavity.

We chose to build a monolithic Fabry-Pérot cavity. In this case, the Pound-Drever locking technique is well suited to mode-lock the laser frequency on a resonant frequency of the cavity. A first prototype of a non-monolithic low Finesse Fabry-Pérot cavity ($F = 1700$) has been described in our previous paper [6]. This prototype was mainly used to design and operate an efficient and robust electronics for the Servo-loop control [11]. The Fabry-Pérot cavity of the TJNAF Compton polarimeter uses the same laser and the same opto-electronics feedback system. We will just mention the slight tunings and improvements which were made to cope with the narrower bandwidth of the cavity ($\Delta\nu_{cav} = 6.8$ kHz) and the accelerator environment.

3.1 The High Finesse monolithic Fabry-Pérot cavity

3.1.1 Description

For the highest luminosity of Compton scattering, the photon beam size at the CIP has to be close to but greater than the electron Gaussian beam radius which is estimated around $\sigma_e \approx 70$ μm. When mode-locked on its fundamental mode, the Fabry-Pérot cavity generates an amplified circular Gaussian beam whose smallest transverse dimension, called the waist, is located at the center of the cavity. The waist radius $\omega_{\gamma,0}$ is measured at $\frac{I_{max}}{e^2}$ and is given by $\omega_{\gamma,0}^2 = 4\sigma_{\gamma,0}^2 = \frac{\lambda L}{2\pi}\sqrt{\frac{1-g}{1+g}}$.

For a monolithic Fabry-Pérot cavity, the two High-Reflectivity mirrors are placed at each side of a high-precision mechanical spacer. The relative position and orientation of the mirrors is fixed by the relative position and orientation of the two sides of the spacer.

We chose to build a cavity of $g = -0.7$ with $R = 0.5$ m and $L = 0.85$ m whose waist radius is therefore $\sigma_{\gamma,0} = 123$ μm. The high-reflectivity cavity mirrors, M_{ce} and M_{cs}, are made of dielectric quarter-wave layers of alternate Low refractive index (SiO_2) and High refractive index (Ta_2O_5) amorphous deposits on a super polished 10 mm diameter silica substrate. We made 11 mirrors at the IN2P3/IPNL/SMA (Villeurbanne, France) using Double Ion beam Sputtering (or DIBS). These mirrors were measured by the manufacturer with an average transmittivity $T = 121 \pm 5$ ppm, an average diffusion $D =$

6 ± 2 ppm and an average absorption $A < 2$ ppm. The two mirrors of the cavity are chosen with close properties and we will assume they have the same transmittivity T and the same total losses $P = A + D$.

The spacer has been designed to enable vacuum pumping, limit the mechanical vibrations of the structure and let the electron beam go through. The designed crossing angle of 23 mrad was chosen to ensure a 5 mm safety distance between the electron beam and the mirrors' edge. The specifications of the spacer are of the highest quality produced commercially, especially in terms of parallelism of the two faces of the spacer (≤ 300 μrad). A first prototype has been successfully tested at Saclay. The final design is shown on figure 3. Both the prototype and the final cavity spacer were manufactured by the MECALIM company at Brives (France) [12].

The mirrors of the cavity are mounted on the spacer in a Class 100 clean room and are kept protected from dust until the connection to the chicane beam pipe is completed.

3.1.2 Mode-locking

For Pound-Drever phase locking, the frequency of the laser is modulated at 928 kHz by applying a sinusoidal voltage of 20 to 40 mV on the Laser piezoelectric actuator which also provides the FAST control of the laser frequency. For larger detuning, a Peltier module commands the Nd:YAG crystal's temperature for a SLOW frequency control. The detuning signal used by the feedback loop is then proportional to the phase of the laser beam reflected by the cavity.

The reflected beam is separated from the incident beam using a polarizing beamsplitter cube (figures 4 and 6). It is then collected by a Spectralon 2" Integrating sphere and the signal is read by a fast Si photodiode (PDR) which is mounted on an exit port of the sphere. This ensures to keep a good collection of the reflected beam during coupling optimization. The sphere also acts as an equivalent optical density of $OD \simeq 2$ that makes the PDR operate in its linear regime.

The feedback loop electronics builds the detuning signal after a current-voltage conversion, filtering (SERVO), demodulation and amplification of the PDR current ([6,11]). To ensure the convenient loop stability, the three stages of the SERVO controller have been adapted to the narrow bandwidth of the cavity. Both the search of a resonant frequency and the closing of the feedback loop are automatic. The mode-locking system is thus fully self-governing to react in a few seconds to an untimely unlock of the cavity or to automatically retrieve the build-up power after a photon beam shutdown or a photon beam polarization reversal (see section 3.3).

For a given Fabry-Pérot cavity design the maximum gain of the power build-up is $G_{max} = \frac{T}{(P+T)^2}$. The actual gain, and thus the actual power available for Compton scattering, is $G = \alpha_{00} G_{max}$ where α_{00} is the transverse fundamental mode coupling ratio and represents the amount of primary power actually amplified in the fundamental mode. To get α_{00} as high as possible, the injected primary photon beam must be as close as possible to the amplified photon beam in shape and orientation.

Note that we have an unavoidable coupling loss in the two modulation side bands used for Pound-Drever locking. It has been measured to be less than 2 % depending on the amount of modulation.

3.2.1 Injected photon beam shape coupling

The laser delivers an elliptical Gaussian beam for which the dimensions have been measured by a beam sampling technique using a Dual-Slits scan head from the PHOTON company with a 10 μm precision. The beam radius at 500 mm from the exit of the laser head are $\omega_x = 680$ μm and $\omega_y = 870$ μm respectively in the horizontal and vertical plane.

A first AR coated convergent lens $f_1 = 400$ mm is used to get a measured $\omega_x = 605$ μm by $\omega_y = 825$ μm collimated beam at the quarter-wave plate location in case of the future use of a Pockels Cell.

We have to focus the beam at the CIP located 2.905 m from the laser exit with a final dimension close to $\omega_{\gamma,0}$. Taking into account the equivalent focal length $f_4 = -1.087$ m of the entrance cavity mirror, Gaussian beam calculations lead to the use of a telescope composed of two AR coated lenses, the first one divergent with focal length $f_2 = -50$ mm and the second one convergent $f_3 = 200$ mm. A fine tuning of the lenses' position focuses the beam 11 cm upstream of the CIP with a measured beam size of $\omega_x = 205$ μm by $\omega_y = 150$ μm (see figure 5). When the entrance cavity mirror is placed, the photon beam dimensions at the CIP are thus theoretically $\omega_x = 210$ μm and $\omega_y = 285$ μm, which can not be measured with our PHOTON scan head because of the very low power transmitted ($\sim$ 30 μW). An unavoidable 3 % coupling loss is awaited because of this ellipticity.

3.2.2 Injected photon beam orientation coupling

When mode-locked on its fundamental mode, the Fabry-Pérot cavity generates an amplified Gaussian beam which is aligned on the optical axis of the cavity.

A periscope made of two remote controlled steering mirrors M_1 and M_2 is used to accurately align the primary photon beam with respect to the optical axis of the cavity (see figure 4). The average angular resolution has been measured close to 10 μrad.

Without the cavity between the input and output stands (see figure 3), the beam is first accurately aligned on the middle of the 12.5 mm diameter steering mirrors M_e and M_s with the help of two 4 cell photodiodes placed in transmission of the mirrors. The Fabry-Pérot cavity is then placed and the beam pipe closed. The incident and reflected photon beams are made coincident on the mirror M_{r2} seen by a CCD camera with the help of the periscope. At this stage, we usually observe high-order transverse modes and a weak fundamental mode. With the incident beam mode-locked on this weak fundamental mode, we finally get the maximum intra-cavity power with slight movements of the incident beam (< 100 μrad) that maximize the output power measured by the integrating spheres S_1 and S_2. This procedure is fully automated. We routinely get a coupling ratio α_{00} close to the upper limit of 95 %.

3.3 Photon beam polarization

3.3.1 Polarization shaping and transport to the CIP

A Faraday Isolator with a 36 dB measured isolation protects the laser from reflected light. The 1/300 linear polarization of the laser beam is first purified (up to 1/100 000) by the output polarizer of the isolator. It is then rotated with a half-wave plate to be perfectly aligned with the direction of transmission of the laser polarizing beamsplitter (chosen vertical). It is finally transformed to a circular polarization with a remote controlled quarter-wave plate.

Two pairs of identical dielectric mirrors whose plane of incidence are orthogonal within 1^o (M_1 - M_{r2} and M_2 - M_e) propagate the circular polarization with minimal distortion. With this compensated scheme, we managed to get a 99.7 % left circular and a 99.6 % right circular polarization at the entrance of the cavity (exit of M_e). This has been obtained for an angle between the linear vertical input polarization and the fast axis of the quarter-wave plate of respectively 50^o counterclockwise and 51^o clockwise.

3.3.2 On-line output polarization measurement

The photon beam polarization is measured on-line at the exit of the cavity after the pair of compensated mirrors M_s - M_3. A Harmonic Beam Sampler (HBS) is used to diffract the beam at $\sim 10^o$ into two first order beams, each one containing 1 % of the incident beam. A CCD camera and a fast Hamamatsu Si

photodiode are placed on the path of these two diffracted beams. The first one allows to view the amplified beam shape and the second one is used for decay time measurements (see section 3.4). The central transmitted beam carries 97.4 % of the incident power and its polarization is preserved within 0.1 %. This polarization is eventually measured by the combination of a Wollaston Calcite prism and a Quarter-Wave plate whose fast axis is accurately oriented at 45° with respect to an optical axis of the prism. The relative proportion between the two calibrated beam powers P_{S_1} and P_{S_2} transmitted by the Wollaston prism is directly linked to the Degree Of Circular Polarization by $P_\gamma^{output} = \frac{P_{S_2} - P_{S_1}}{P_{S_2} + P_{S_1}}$.

To measure I_{S_1} and I_{S_2} we use an InGaAs photodiode placed at an exit port of a 2" Spectralon integrating sphere (LABSPHERE Company). The photodiodes have been calibrated by the manufacturer (NEWPORT company) and a powermeter reads the scattered flux P_{m_2} and P_{m_1} seen by the photodiodes. We have calibrated the overall response of the two Sphere + photodiode systems with a calibrated powermeter from the COHERENT company. Their response is linear up to 700 mW incident power with a calibration coefficient K_{S_i} given by $P_{S_i}[mW] = K_{S_i}.P_{m_i}[\mu W]$ (table 1).

The Quarter-Wave plate is motorized and we can derive the 4 Stokes parameters of the photon beam from the measurements of P_{S_1} and P_{S_2} for at least three different orientations of the fast axis. This complete characterization of the slightly elliptical polarization (orientation and DOCP) will be necessary to get the absolute photon beam polarization at the CIP.

3.4 Performances of the Fabry-Pérot cavity

The intra-cavity power is given by $P_{cav} = \alpha_{00} G_{max} P_i = \frac{P_t}{T}$ where P_i (resp. P_t) is the injected power at the entrance of the cavity (resp. the power at the exit of the cavity). The injected power P_i is deduced from the power measurements P_{S_e} in transmission of the mirror M_1 (InGaAs photodiode + integrating Sphere) with $P_i[mW] = K_e.P_{S_e}[\mu W]$. The output cavity power P_t is deduced from the power measurements P_{S_1} and P_{S_2} by $P_t[mW] = K_t.(P_{S_1}[mW] + P_{S_1}[mW])$. The calibration coefficients K_e and K_t have been determined for the two circular polarizations and are given in table 1.

Although the loss ratio $\beta = \frac{A+D}{T}$ has been measured by the manufacturer ($\beta \approx 0.058$), we regularly measure it in case of mirror pollution during the installation of the cavity. We also need to monitor it on-line to detect a possible damaging of the mirrors (pollution or radiation damage).

Neglecting the power carried by the modulation side bands, one can show that

α_{00} and β can be derived from the following equations:

$$\beta = \frac{1}{2}\left(\frac{P_i}{P_t}\left(1 - \frac{P_r^{cL}}{P_r^{oL}}\right) - 1\right) \quad (1)$$

$$\alpha_{00} = \frac{P_t}{P_i}(1+\beta)^2 \quad (2)$$

where P_r^{cL} and P_r^{oL} are the powers reflected by the cavity with the feedback loop respectively closed and opened. The ratio $\frac{P_r^{cL}}{P_r^{oL}}$ is measured on line by the ratio $\frac{V_{PDR}^{cL}}{P_{PDR}^{oL}}$ where V_{PDR}^{cL} and V_{PDR}^{oL} are the PDR voltages with closed and opened loop respectively.

Finally, for a High-Finesse cavity ($F > 10000$), the Finesse is linked to the total losses and transmittivity of the mirrors by $P + T = \frac{\pi}{F} = \frac{L}{c.T_d}$ where T_d is the decay time of the cavity. The cavity mode-locked on its fundamental mode, we measure the experimental cavity decay time by shutting off the diode pumping of the laser (Standby mode) and recording the PDR or PDT voltage on a fast digital oscilloscope. T_d is obtained by fitting the convolution of the theoretical exponential of the emptying of the cavity by the experimental exponential decay of the laser itself (decay time ≈ 6 μs).

The results are summarized in table 2. The performances of the system are similar in the two circular polarizations. An average of 92.5 % of the 229 mW of injected power is coupled in the fundamental mode of the cavity. The intra-cavity power is close to 1.6 kW, i.e 0.85 MW/cm^2 power density at the CIP. The power density on the cavity mirrors is 125 kW/cm^2 which is below their supposed limit (≤ 1 MW/cm^2 for a continuous wave). An example of recording of the intra-cavity power with a 10 μA electron beam crossing (figure 7) shows a 3 % stability over 10 hours.

We are currently working on the absolute calibration of the photon beam polarization at the CIP. The difficulty comes from the inherent impossibility to perform a measurement at the CIP because of the power buildup process and from the non accessibility for on line optical measurements inside the central vacuum beam pipe. For the time being, the polarization measurements with and without the cavity are given in table 2. The measured output polarization P_γ^{out} is stable at 0.05 % (see figure 7).

4 Preliminary analysis of Compton events

This chapter is dedicated to a preliminary analysis of the Compton events acquired with the complete polarimeter setup. We finally derive an experimental longitudinal integrated asymmetry which is the first step toward an electron beam polarization measurement.

4.1 Beam Crossing

Once the background is lowered to an acceptable value, i.e 400 Hz at 2 μA in the central crystal of the photon detector, the electron beam is moved vertically until it crosses the photon beam inside the cavity. Figure 8 displays the counting rates in the central crystal during the scanning procedure. It corresponds to the expected luminosity of the two interacting beams:

$$L_{max}(y) = \frac{1}{\sqrt{2\pi}} \frac{I_e}{e} \frac{P_L \lambda}{hc^2} \frac{G}{\sqrt{\sigma_e^2 + \sigma_\gamma^2}} \frac{(1 + cos\alpha_c)}{sin\alpha_c} \exp\left(-\frac{y^2}{2(\sigma_e^2 + \sigma_\gamma^2)}\right) \quad (3)$$

where y is the vertical distance between the two beams, I_e is the electron beam intensity, P_L is the laser power, λ is the laser wavelength, G is the amplification gain the optical cavity, σ_e and σ_γ are electron and photon beam sizes at the CIP, and α_c is the crossing angle of the two beams. The photon beam size defined by the cavity is $\sigma_{\gamma,0} = 123\ \mu m$ at the CIP. Using equation 3, we found the electron beam size to be $\sigma_e \approx 75\ \mu m$, which is close to the accelerator specifications ($\sigma_e \approx 100\ \mu m$).

The final magnet settings were determined by the maximum luminosity of the position scan. The counting rate variations correlated to the cavity laser power are shown in figure 9, as the locking system was turned on and off. We observed an excess of $2.5 kHz/\mu A$ in the counting rate when the cavity is mode-locked. It is in agreement with the rate determined using equation 3.

4.2 Background subtraction

Figure 10 shows the raw energy spectrum deposited in the photon calorimeter. To construct the Compton energy spectrum, background has to be subtracted. This background is mainly due to the Bremsthralung radiation emitted by electrons in the residual gaz and at the edges of the apertures located close to the mirrors holders (see figure 3). Background is measured by turning off the cavity. During the experiment, the signal over background ratio was $3 < \frac{S}{B} < 20$. The ADC spectrum obtained with background events is then substracted from

the raw spectrum when the cavity is on. The normalization of the two spectra is performed in the high energy region where no Compton scattering is expected and where the spectra have the same shape.

4.3 Experimental asymmetry

The helicity reversal rate of the electron beam produced at CEBAF is 30 Hz. Using the total counting rates in the central crystal of the photon detector, one can construct a pulse-by-pulse asymmetry from the two opposite helicity states. Counting rates are normalized to the beam intensity and the asymmetry is corrected for the dilution due to the background. Figure 11 shows the pulse by pulse asymmetry distributions, A_{right} and A_{left}, for the two photon polarization states. The average result is $A_{right} = -1.14 \pm 0.02$ % and $A_{left} = 1.18 \pm 0.02$ %.

A statistical accuracy of 1 % is achieved within one hour. As expected, the experimental asymetry flips sign with the photon helicity.

To extract the electron beam polarization, the experimental asymmetry will be compared to the theoretical cross section asymmetry $< A_{th} >$ in the corresponding energy range. Determination of the beam polarization is sensitive to :

- the energy threshold E_0 above which photons are detected in the calorimeter in order to compute $< A_{th} >$ given by :
$$< A_{th} >= \frac{\int_{E_0}^{\infty} A_{th}(E) \frac{d\sigma}{dE} dE}{\int_{E_0}^{\infty} \frac{d\sigma}{dE} dE},$$
- the energy calibration and resolution of the detector,
- false asymmetries due to the helicity correlated beam parameters, such as position, angle, shape, etc ...

This will provide a monitoring of relative variations of the beam polarization with an uncertainty less than 2% and an absolute determination of the polarization with an uncertainty of 3%.

5 Conclusion

We have successfully designed and operated a new kind of Compton polarimeter at Jlab which uses a High Finesse Fabry-Pérot cavity as a high power photon source. The TJNAF Hall A polarimeter has been working for six months under beam conditions during the HAPPEX experiment [13] with no noticeable degradation of its performances. This is a remarkable result regarding

the very short distance between the electron beam and the cavity mirrors (5 mm). The Finesse of the cavity is 26000. This corresponds to an equivalent build-up gain of 7300. The photon beam power density at the CIP is therefore 0.85 MW/cm^2.

The preliminary analysis of the Compton scattering events aquired during the first two months of operation is very encouraging. A good signal to noise ratio in the photon detector has been achieved ($3 < \frac{S}{B} < 20$) and a preliminary analysis of the data lead to an experimental asymetry of $|A_{exp}| = 1.16 \pm 0.2$ %. We are currently studying systematic errors which is the next step towards the electron beam polarization measurement : influence of the calibration and resolution of the photon calorimeter on the determination of $< A_{th} >$, false asymmetries due to helicity correlated beam parameters, and absolute calibration of the photon beam polarization at the interaction point.

6 Acknowledgments

We would like to thank the technical staffs of IN2P3 and TJNAF for their contributions. We are grateful to J. Feltesse and C. W. de Jager for their constant support.

References

[1] L. Cardman, Nuclear Physics News, Vol.6, No. 4 (1996) 18.

[2] I. Passchier et al., Nucl. Instr. and Meth. A414 (1998) 446.

[3] M.Woods et al, Proc. SPIN96 Conference, World Scientific, Singapore, 1996, p. 843.

[4] D. P. Barber et al., Nucl. Instr. and Meth. A329 (1993) 79.

[5] G. Bardin et al., Conceptual Design Report of a Compton Polarimeter for CEBAF Hall A, Internal Report DAPNIA-SphN-96-14 (1996).

[6] J.P. Jorda et al., Nucl. Instr. and Meth. A412 (1998) 1.

[7] HAPPEX Collaboration, Phys. Rev. Lett. 82 (1999) 1096.

[8] C. Prescott, SLAC internal report, SLAC TN 73 1.

[9] D. Neyret et al., A photon calorimeter using lead tungstate crystals for the Cebaf hall A Compton polarimeter, to be published in NIM A.

[10] EPICS, Experimental Physics and Industrial Control Systems. Web site : http://www.aps.anl.gov/xfd/SoftDist/Welcome.html.

[11] J.P. Jorda, Mise au point d'une cavité Fabry-Pérot pour la polarimétrie Compton, thèse de doctorat de l'université Paris 6, soutenue le 31 octobre 1997.

[12] MECALIM, zone industrielle de Beauregard, 19100 Brives, France.

[13] HAPPEX Collaboration, to be submitted to Phys. Rev. Lett.

List of Tables

List of Figures

Calibration Coefficient	Left polarization	Right polarization
$K_{S_1}(mW/\mu W)$	0.238 ± 0.002	0.238 ± 0.002
$K_{S_2}(mW/\mu W)$	0.268 ± 0.002	0.268 ± 0.002
$K_e(mW/\mu W)$	236 ± 3	244 ± 3
K_t	1.162 ± 0.002	1.152 ± 0.002

Table 1

Calibration coefficients for the Photon beam power measurements.

	Left polarization	Right polarization
Cavity length (m)	0.85 ± 10^{-4}	0.85 ± 10^{-4}
Vacuum (Torr)	$\simeq 10^{-8}$	$\simeq 10^{-8}$
Injected Power P_i (mW)	229 ± 3	229 ± 3
Modulation amplitude (mVpp)	20	20
PDR signal with opened loop (mV)	874 ± 8	878 ± 8
PDR signal with closed loop (mV)	118 ± 8	107 ± 10
PDR background signal (mV)	36.4 ± 0.5	36.4 ± 0.5
Coupling ratio $\alpha_{00} = \frac{P_t}{P_i}(1+\beta)^2$	0.918 ± 0.012	0.930 ± 0.014
Loss ratio $\beta = \frac{A+D}{T}$	0.149 ± 0.013	0.138 ± 0.013
Cavity decay time T_d (μs)	23.5 ± 0.5	23.5 ± 0.5
Cavity Finesse $F = \pi \frac{T_d c}{L}$	26040 ± 550	26040 ± 550
Cavity Bandwidth $\Delta\nu_c = \frac{FSR}{F}$ (kHz)	6.8 ± 0.14	6.8 ± 0.14
Mirror transmittance T (ppm)	105 ± 2.5	106 ± 4
Mirror total losses $P = A + D$ (ppm)	16 ± 1	15 ± 1
Cavity maximum Gain $G_{max} = \frac{T}{(P+T)^2}$	7210 ± 200	7290 ± 200
Output powers		
P_{s1} (mW)	0.646 ± 0.003	142.1 ± 0.4
P_{s2} (mW)	136.2 ± 0.4	1.031 ± 0.004
Injected Polarization $P_\gamma^{injected}$ without cavity	0.997 ± 0.005	-0.996 ± 0.005
Output polarization P_γ^{out} without cavity	0.989 ± 0.005	-0.993 ± 0.005
Output polarization P_γ^{out} with cavity	0.991 ± 0.005	-0.986 ± 0.005
Cavity output Power P_t (mW)	159.0 ± 1.5	165 ± 1
Intra-cavity Power $P_{cav} = \frac{P_t}{T}$ (W)	1515 ± 50	1550 ± 50
Intra-cavity Power $P_{cav} = \alpha_{00} G_{max} P_i$ (W)	1545 ± 50	1580 ± 50
Estimated intra-cavity Power P_{cav} (W)	1530 ± 50	1565 ± 50

Table 2

Main features of the Fabry-Pérot cavity (measured with electron beam crossing)

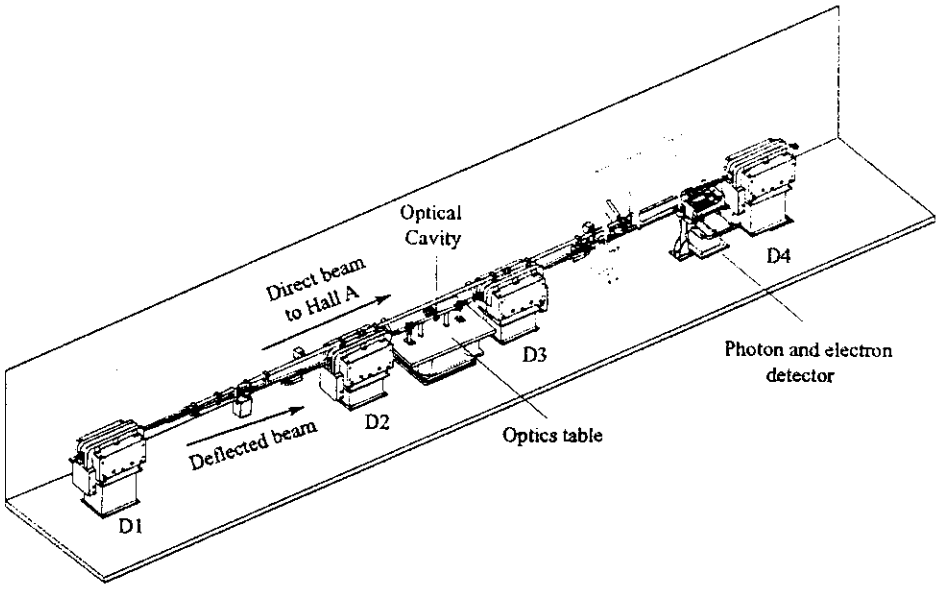

Fig. 1. *3D view of the TJNAF Hall A Compton Polarimeter.*

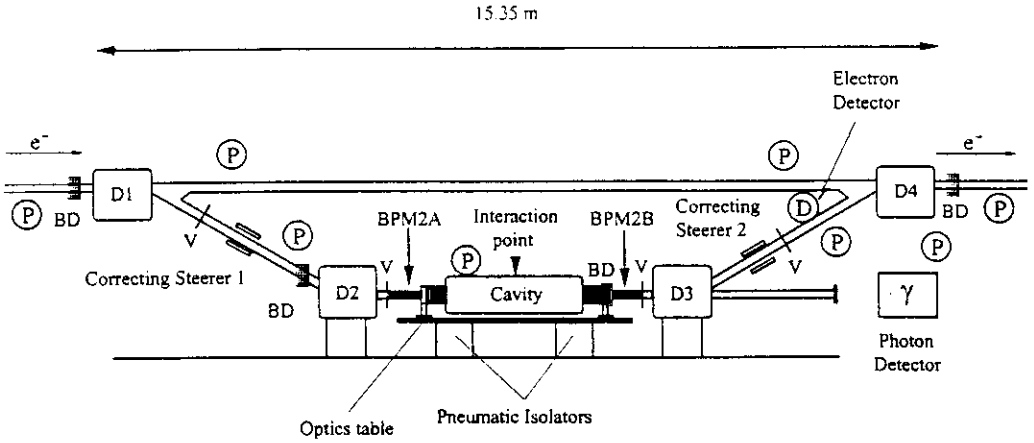

Fig. 2. *Detailed side view of the TJNAF Hall A Compton Polarimeter. P : Ionic pumps, BD : Beam Diagnostics, V : Pneumatic Vacuum gates.*

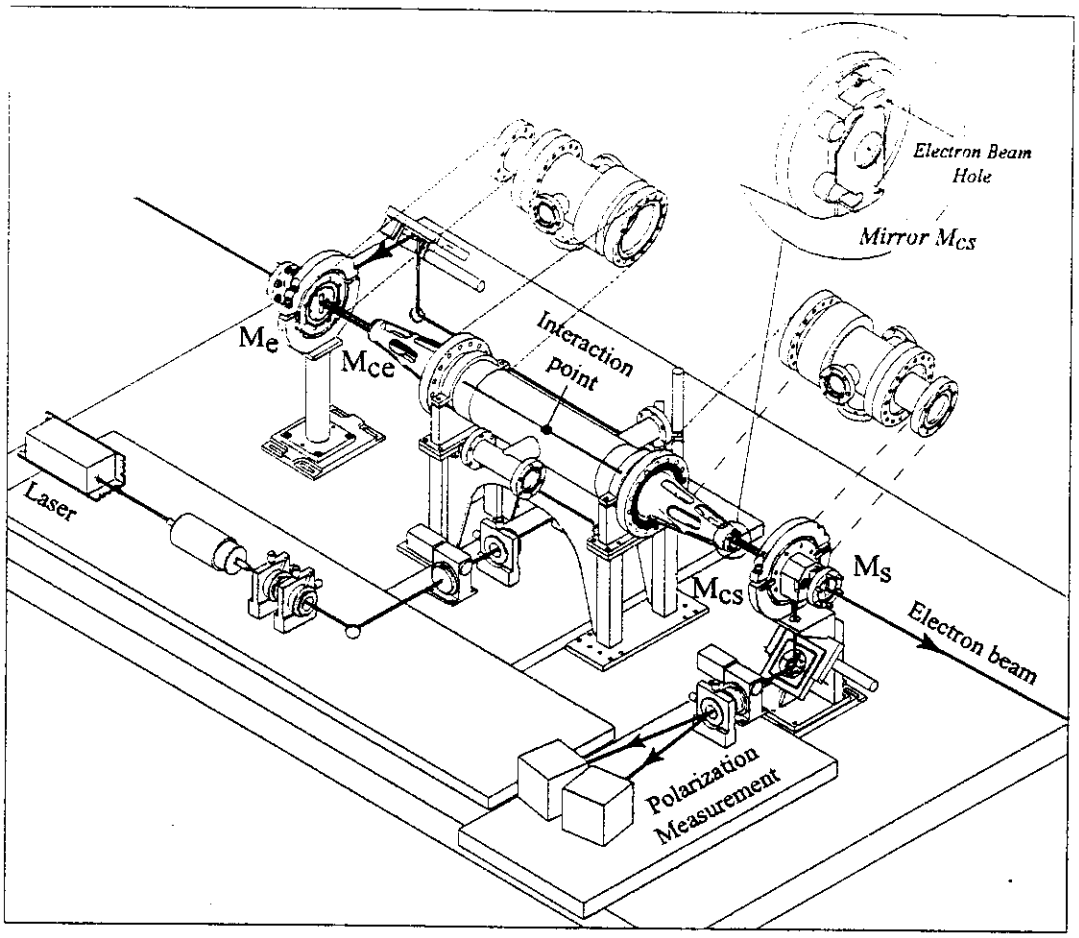

Fig. 3. *3D view of the optics table with the monolithic cavity (beam pipe opened).*

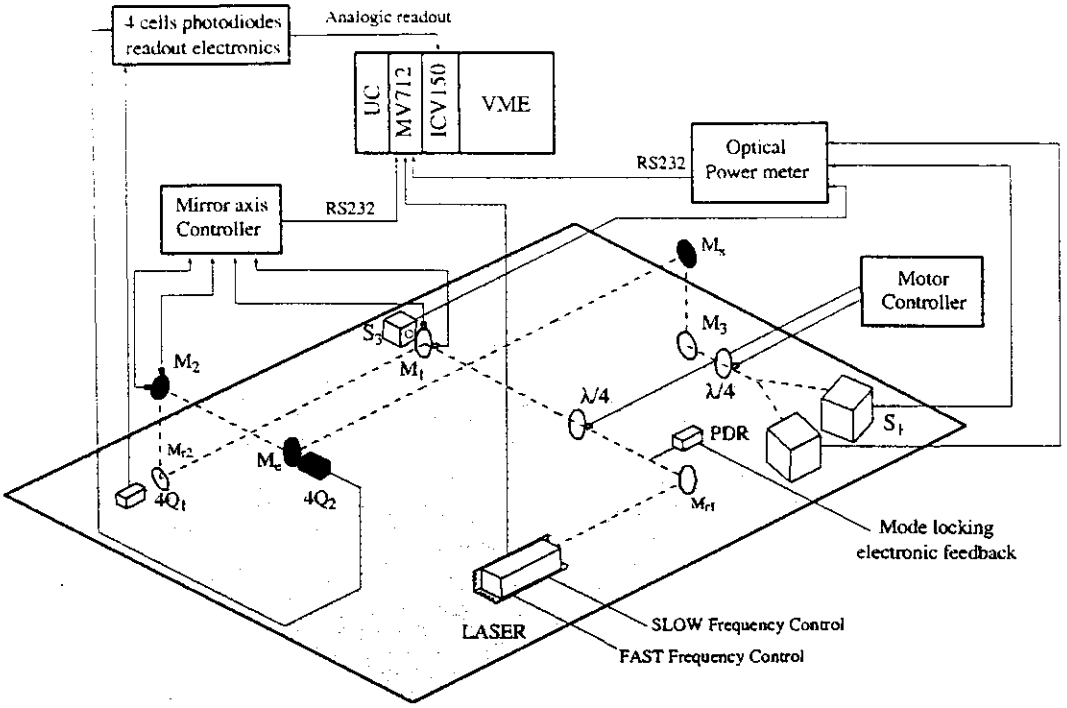

Fig. 4. *Functional view of the Fabry-Pérot cavity system.*

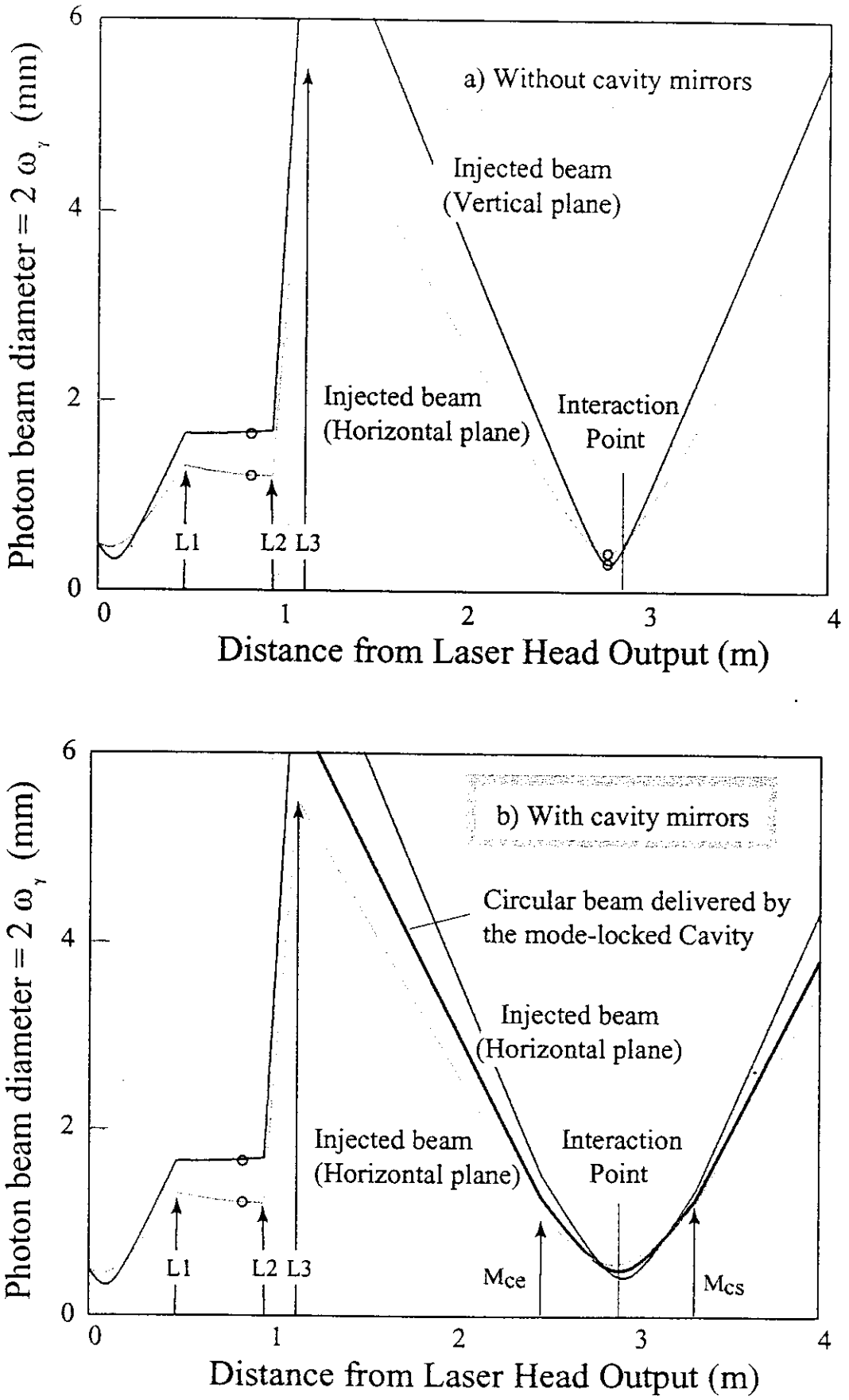

Fig. 5. *Calculated and measured Photon beam diameter ω_γ as a function of the distance along the beam path from the laser head output. The black (resp. gray) curves correspond to the Vertical (resp. Horizontal) plane in the cavity. The circles are the measured beam diameters.*

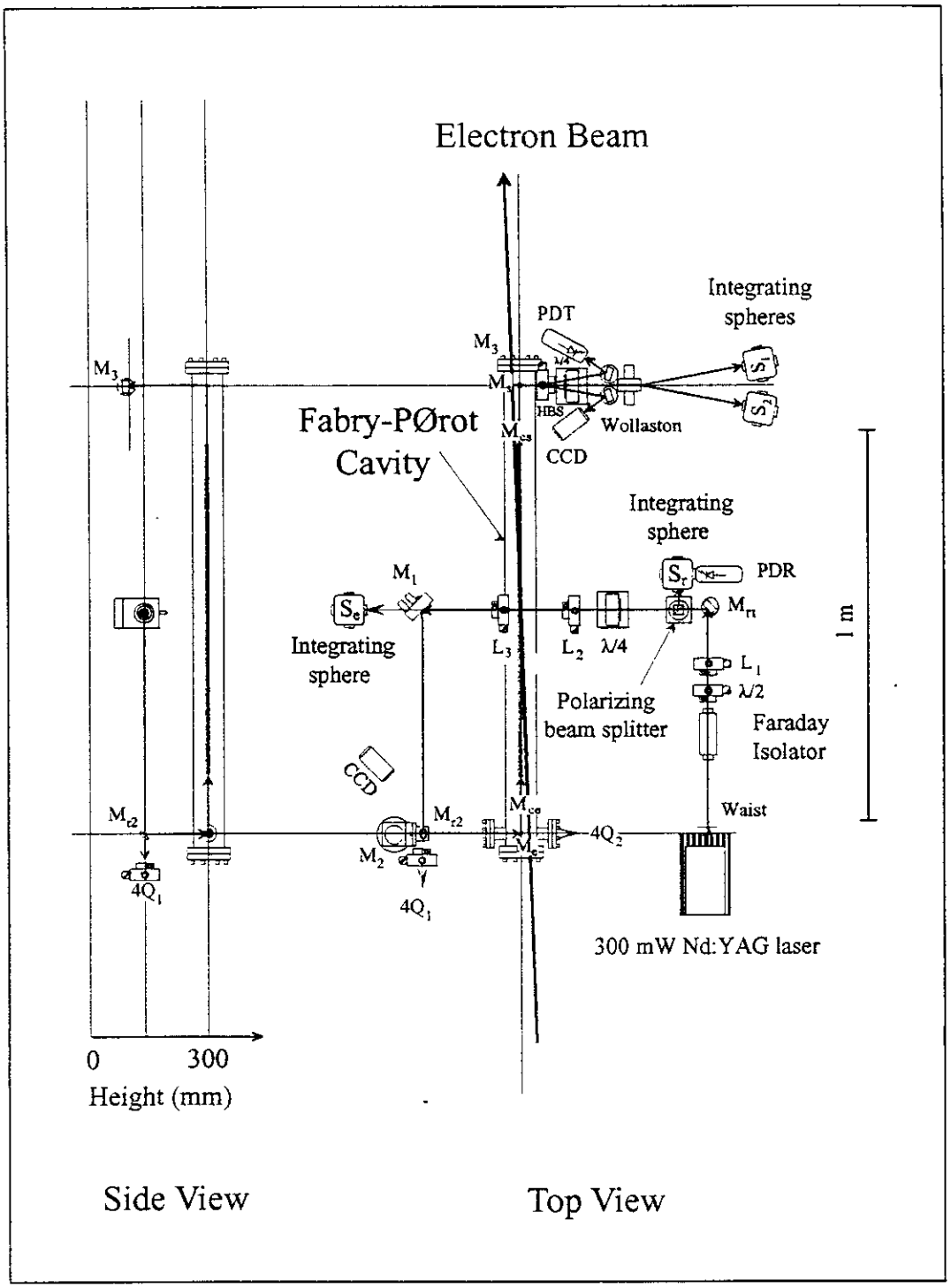

Fig. 6. *Layout of the optics table in the hall A tunnel (top and side views).*

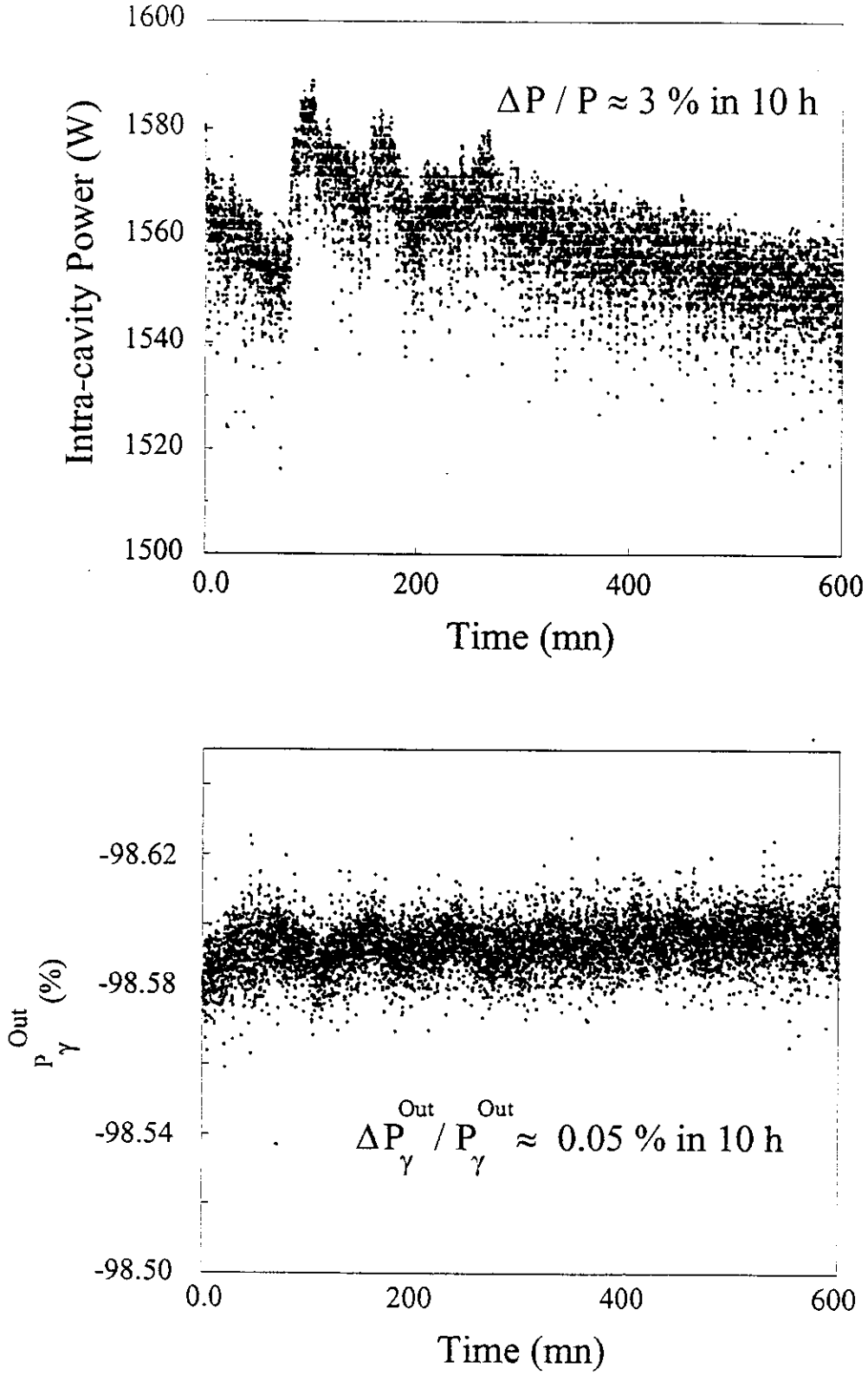

Fig. 7. *Intra-cavity power (top) and output photon beam polarization (bottom) over a 10 hours period with a 10 μA electron beam.*

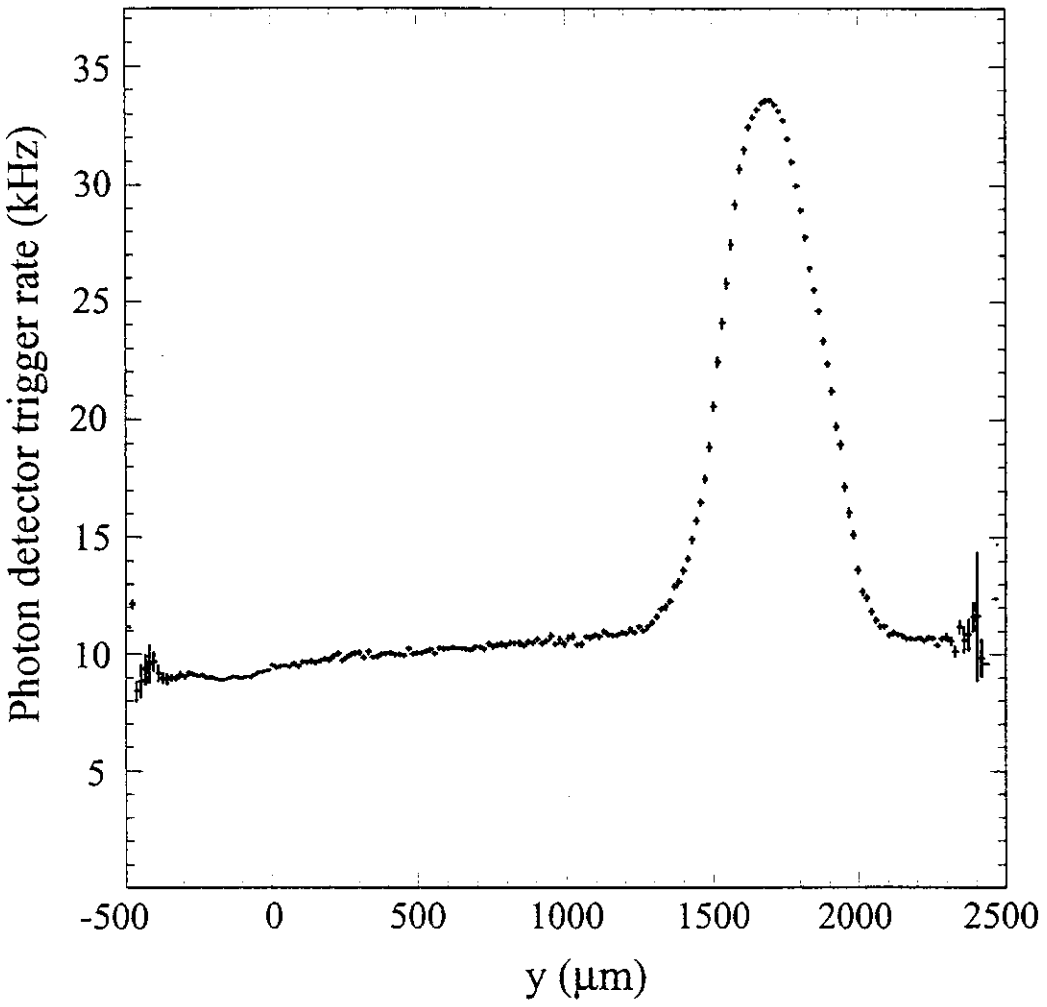

Fig. 8. *Counting rates in the central crystal of the photon detector as a function of the vertical distance y between the two beams. The electron beam current is* 10 μA *and the intra-cavity photon power is 1.6 kW.*

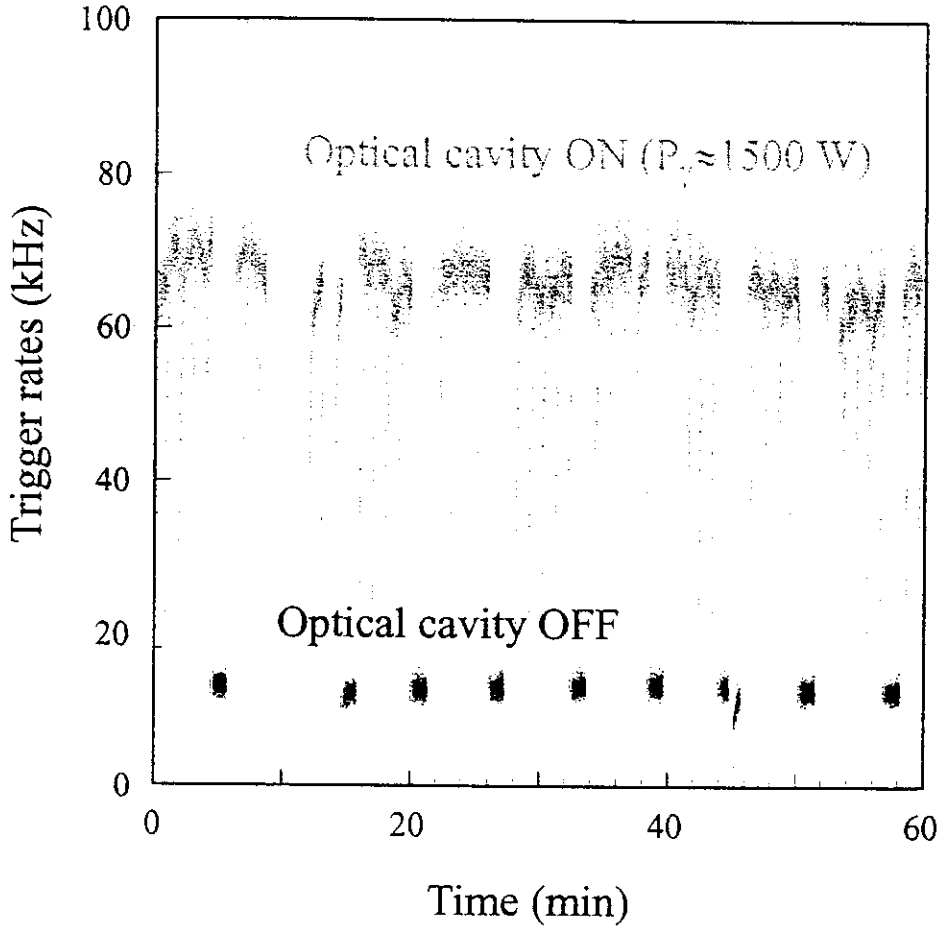

Fig. 9. *Correlation between the measured counting rates in the photon detector and the intra-cavity power. The electron beam conditions are those of the HAPPEX experiment, E=3.355 GeV and* $I_e = 40\mu$ *A.*

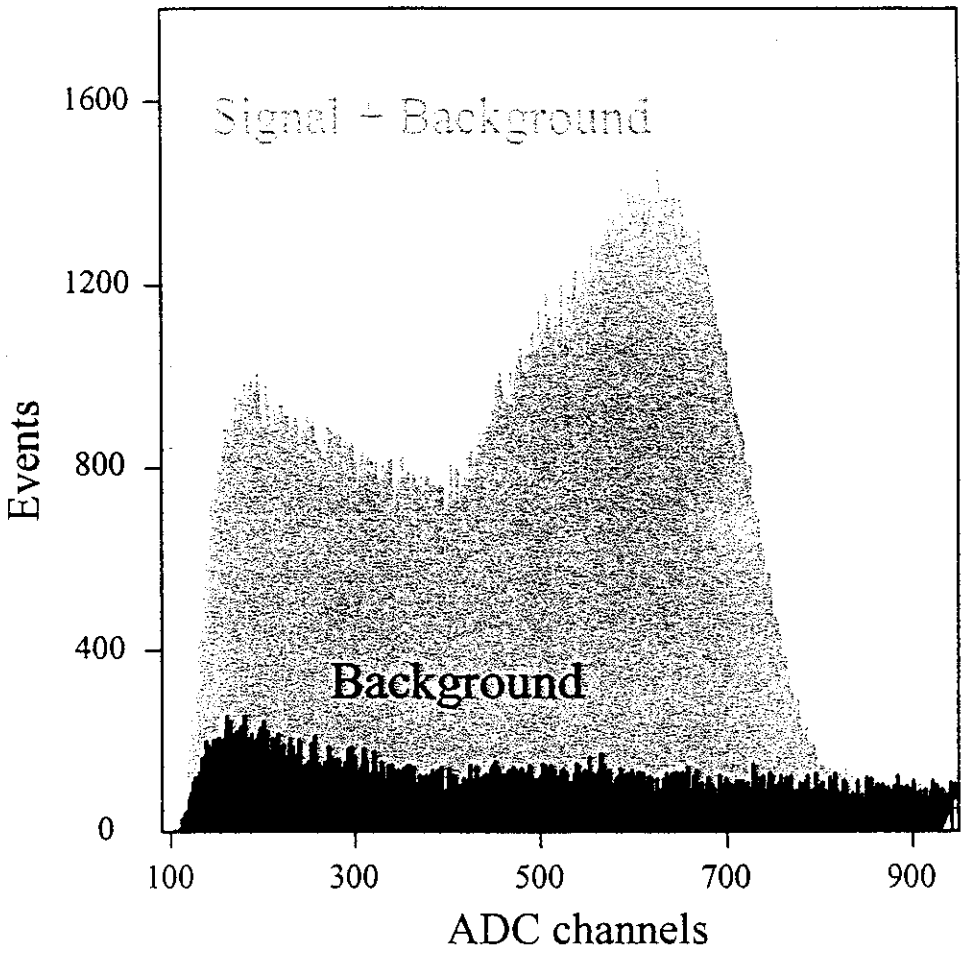

Fig. 10. *Background subtraction : normalized Signal+Background and Background spectra. The Compton edge is around ADC channel 500 corresponding to an energy about 190 MeV of the backscattered photon.*

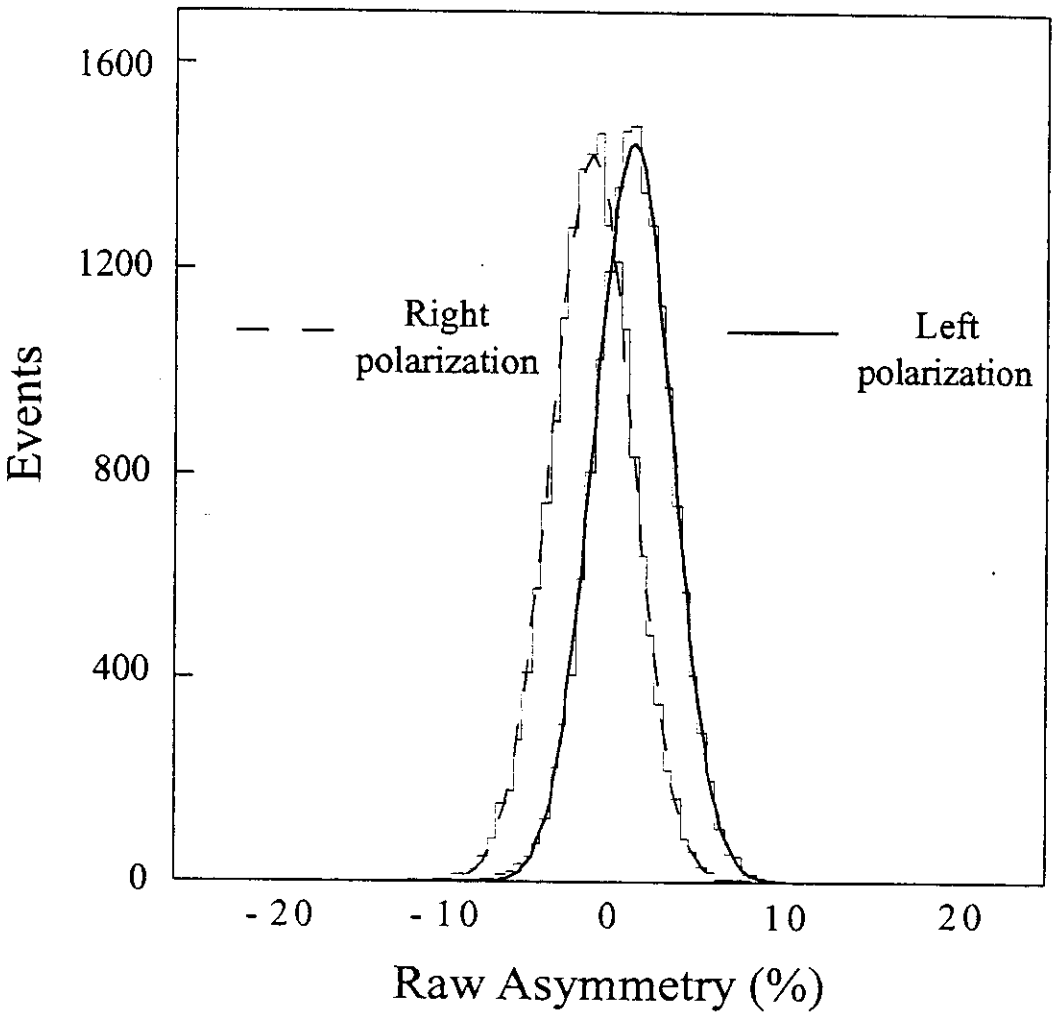

Fig. 11. *Distribution of the pulse-by-pulse experimental asymmetry obtained for the two polarization states of the photon beam.*